ISSN: 0123-3033 – ISSN-e: 2027-8284

INGENIERIA Y COMPETITIVIDAD
REVISTA CIENTÍFICA Y TECNOLÓGICA

Vol. 25 No. 1-2023 - DOI: 10.25100/iyc.25i1.11832

MATERIALS ENGINEERING

# Evaluation of adhesion and corrosion wear resistance of biobased polymers derived from linseed oil deposited on Fe-Zn sheets

INGENIERÍA DE MATERIALES

# Evaluación de la adherencia y de la Resistencia al desgaste por corrosión de polímeros biobasados de aceite de linaza depositados en placas de Fe-Zn

**Jorge Tello-Gonzalez[1], Susana Hernández-López[1], Enrique Vigueras-Santiago[§1] David A. Gonzalez-Martinez[1], Gonzalo Martínez-Barrera [1]**

[1] *Universidad Autónoma del Estado de México,* Laboratorio de Investigación y Desarrollo de Materiales Avanzados (LIDMA), Facultad de Química. *México*

jtellog012@alumno.uaemex.mx, shernandezl@uaemex.mx,

evigueras@uaemex.mx, dgonzalezm384@alumno.uaemex.mx, gonmar@uaemex.mx

Tello-González J, Hernández-López S, Vigueras-Santiago E, González-Martínez D, Martínez-Barrera G. Evaluación de la adherencia y de la Resistencia al desgaste por corrosión de polímeros biobasados de aceite de linaza depositados en placas de Fe-Zn. Ingeniería y competitividad, 2023, 25(1);e- 20811832. https://doi.org/10.25100/iyc.v25i1.11832

**Recibido**: 16 de diciembre de 2021 – **Aceptado**: 05 de junio de 2022

## Abstract

The objective of this paper is to study adherence and corrosion wear resistance of biobased polymers derived from epoxidized linseed oil (ELO) deposited on galvanized iron sheets. The adhesion and anticorrosive properties of the pure epoxy resin (ELO) were compared with those that contained bisphenol A (BFA) and carbon black (CB), which were polymerized by oxirane ring opening catalyzed by aluminum triflate (ATf). Fourier Transform Infrared Spectroscopy (FTIR) confirmed the formation of the different biobased polymers as coatings. To evaluate the performance to the corrosion resistance each coating was tested to adhesion and accelerated weathering within a salt spray chamber. The use of BFA provided greater adhesion than pure ELO coatings. Additionally, the addition of small loads of CB improved the appearance, adhesion, and durability of the coating, thus decreasing the corrosion of the

galvanized sheets. Finally, the interactions that occur at the interface between the different polymeric matrices and the substrate surface, which allow improving the corrosion resistance were analyzed.

***Keywords:*** *Epoxidized linseed oil, Carbon black, Coatings, Adhesion, Corrosion.*

## Resumen

El objetivo de este trabajo es estudiar la adherencia y la resistencia al desgaste por corrosión de polímeros derivados del aceite de linaza epoxidado (ELO), depositado sobre láminas de hierro galvanizado. Se compararon las propiedades de adhesión y anticorrosivas de la resina epoxi pura (ELO) con aquellas que contenían bisfenol A (BFA) y negro de humo (CB), todas polimerizadas por apertura de anillo de oxirano catalizada por triflato de aluminio (ATf). La espectroscopia infrarroja por transformada de Fourier (FTIR) confirmó la formación de los diferentes polímeros de base biológica como recubrimientos. Para determinar la resistencia a la corrosión, se evaluó la adhesión de cada revestimiento, así como el intemperismo acelerado dentro de una cámara de niebla salina. El uso de BFA proporcionó una mayor adherencia que los recubrimientos ELO puros. Además, la adición de pequeñas cargas de CB mejoró la apariencia, adherencia y durabilidad del revestimiento, disminuyendo así la corrosión de las láminas galvanizadas. Finalmente, se analizaron las interacciones que ocurren en la interfaz entre las diferentes matrices poliméricas y la superficie del sustrato, que permitieron mejorar la resistencia a la corrosión.

***Palabras clave:*** *Aceite de soya epoxidado, Negro de carbono, Recubrimiento, Adherencia, Corrosión.*

## 1. Introduction

In most industries, metal corrosion represents a problem because it affects the mechanical properties of metals, causing detriment to structures and consequently failures in their function and thus having an impact on the economic aspect (1-5).

It has been proposed that the use of polymeric coatings as a protective barrier to mitigate corrosion is the most effective method to extend the useful life of metals. Although the coatings derived from petroleum sources show high anticorrosive performance and higher chemical stability than other coatings (such as metallic coatings), most of them exhibit toxicity problems, causing environmental contamination and health hazards (1, 3, 6, 7).

Thus, research is currently focusing on organic coatings derived from natural sources such as vegetable oils (VO) due to their lower toxicity, biodegradability, renewability, low cost, and so on. Coatings from VO have good anticorrosive properties and are more environmentally friendly; however, they often have lower mechanical properties than their petroleum-based counterparts. Furthermore, the chemical modification of VO through different methodologies, such as amidation, carbonation, and epoxidation, can be used to modify the chemical nature of VO, providing the properties required for specific application (2,6,8-15).

Polymers from epoxy resins are often used as coatings in various applications because of the oxirane ring that is highly reactive and can carry out crosslinking reactions with different agents. These resins exhibit excellent corrosion resistance, are inert to many chemical agents, and are resistant to weathering applications. Additionally, they possess good processability and adherence to different substrates. Thus, epoxy resins are widely used as adhesives and coatings in composite materials for the automotive, aerospace, naval, and electronic industries (1,16-18).

Several studies showed that VO epoxy resins have been modified with various crosslinking agents, reinforcements, catalysts, or varying reaction parameters to obtain versatile materials with specific characteristics and a wide range of

applications. The most common curing agents are amines, amides, anhydrides, polyacids, metal halides, esters, aromatics, aliphatic, polyols, and so on (17-19). The most common epoxy resin is based on the reaction between bisphenol A (BPA) and epichlorohydrin, which accounts for almost 90% of world production. It is characterized by good heat resistance, electrical insulation, dimensional stability, and chemical resistance; thus, it is used as an industrial material. (1, 17, 19, 20).

Using reinforcing materials is one of the ways to improve the properties of the coatings. Carbon black (CB) is widely used as a filler for polymeric composites in the automotive, cement, pigments, coatings, and so on because it has excellent properties such as heat, chemical and weather resistance, lightweight, electrical conductivity, and low thermal expansion. Moreover, various investigations have shown that the addition of CB enhances the electrical, mechanical, thermal, and tribological properties of epoxy resins (16, 21, 22).

During the polymerization process, epoxy resins can present some drawbacks, such as the formation of by-products when the reaction is carried out at high temperatures and polymer shrinkage if the curing is realized with amines or amides. To mitigate these drawbacks, it has been proposed to use cationic catalysts, which act as Lewis acids because they allow carrying out the curing by homopolymerization. Nevertheless, traditional Lewis acids such as $BF_3$, $TiCl_4$, and $AlCl_3$ are sensitive to moisture and can be deactivated or decomposed in the presence of water (19).

Metal triflates are Lewis acids, which have emerged as an alternative to the existing cationic initiators in various organic reactions, specifically in cationic polymerization. Compared to the conventional ones, metal triflates can be used in catalytic quantities and recycled without significant loss in activity and are stable in water or protic medium. Aluminum trifluoromethanesulfonate ($Al(OTf)_3$) or aluminum triflate (ATf) is considered a convenient Lewis acid because it has no corrosion effect and allows curing reactions of VO epoxy resins to be carried out at low temperatures (23,24). However, there have been few studies on the polymerization of oxirane rings from VO in the presence of crosslinking and reinforcement agents.

Therefore, this study aimed to study the anticorrosive coating potential of a series of resins derived from (a) pure epoxidized linseed oil (ELO), (b) ELO + BFA as a curing agent that could improve the rigidity and adhesion, (c) ELO + CB as a reinforcement filler, and (d) ELO + BFA + CB; all of them were cured in the presence of ATf as a cationic catalyst. To corroborate the structural changes of materials, we used the Fourier Transform Infrared Spectroscopy (FTIR) technique. The coatings were evaluated by adhesion tests on commercial galvanized steel plates as well as corrosion protection tests through accelerated weathering tests.

## 2. Methodology

ELO was synthesized based on the methodology proposed by Dehonor-Márquez et al. (25). The molecular weight (1,007.3 g/mol) and the number of epoxy groups (6.26 per triglyceride molecule) were quantified by Proton Nuclear Magnetic Resonance ($^1$H-NMR) spectroscopy. The catalyst ATf and the crosslinking agent BFA were purchased from Sigma-Aldrich, Co. Vulcan XC72 CB, obtained from Cabot Co., was used without any previous treatment.

FTIR spectra were performed on a Shimadzu FTIR Prestige-21 spectrometer, which has a diamond crystal and a Horizontal Attenuated Total Reflectance (HART) module. The infrared spectra were obtained in absorbance mode, 64

scans, and a resolution of 4 $cm^{-1}$ in the range of 560–4000 $cm^{-1}$. Corresponding to the triglyceride ester group's carbonyl vibration, all FTIR spectra were normalized to the signal at 1736 $cm^{-1}$, as reported by González-Martínez et al. (26).

**2.1 Polymerization of ELO.** The substrates (Fe-Zn sheets) were washed with soap and water, rinsed with acetone, and dried. In a container, 3 g of ELO was added to 10 ml of a 0.01 M ATf solution in acetone, previously prepared. Then, the mixture was stirred and placed in a vacuum desiccator for 3 h. Subsequently, the absence of acetone in the monomer was corroborated by FTIR. The substrates were uniformly coated with the ELO-ATF mixture, and the polymerization was performed by placing the sample in a programmable oven at different temperatures from 50 to 80°C for 30 min. By FTIR, the reaction time (30 min) was established by following the evolution (decreasing until disappearing) of the signal associated with an epoxy ring at 823 $cm^{-1}$.

**2.2. Polymerization of ELO with BFA**. 3 g of ELO was added to 19 ml of a 0.5 M BFA solution in tetrahydrofuran, previously prepared, with a stoichiometric ratio of 1:0.5. It was mixed perfectly, and immediately, 5.85 ml of ATf solution (0.01 M) was added. The mixture was placed in a vacuum desiccator for 1.5 h. Subsequently, the substrate was coated and placed in the oven at the set temperature (50–80°C) for 30 min.

**2.3. Polymerization of ELO with CB.** 15 ml of 1% CB solution in acetone was prepared. Both reagents were mixed. The dispersion was placed in ultrasonic equipment for 1 h. Then, 3 g of ELO and 5 ml of acetone were added to the previous dispersion, and they were stirred for 30 min. Immediately, 10 ml of 0.01 M ATf solution was added, and it was stirred magnetically for 30 min and left in a vacuum desiccator for 24 h. The mixture was placed on the substrate and subsequently in an oven at the set temperature (50–80°C) for 30 min.

**2.4. Adhesion test.** The adhesion test of crosslinked polymers on the galvanized steel plates was performed according to ASTM D3359-02, obtaining the adhesion level of each polymer. Furthermore, the described Method A, also known as the 3M test, was chosen. This method is applicable to finished products, inspections during production, and also inspections before shipment.

**2.5. Accelerated weathering tests**. The conditions were controlled within a salt spray chamber for weathering tests following the ASTM-B117 test. This procedure evaluates the physical appearance of galvanized steel plates coated with different polymers obtained to provide corrosion resistance after 240 h of exposure to extreme conditions within the salt spray chamber (Table 1).

*Table 1*. Salt spray chamber operating conditions

| | |
|---|---|
| **Exposure time** | 240 h |
| **Temperature inside the chamber** | 35 °C |
| **Ratio NaCl saline solution: Distilled water type 4** | 95:5 |
| **Solution density** | 1.027212 $g/cm^3$ |
| **Solution pH** | 7.1 |
| **Sample position** | 20° parallel to mist flow direction |
| **Sample cleaning method at the end of the process** | Sand blast |

*Source: ASTM B117-02*

## 3. Results

As a first step, the epoxidation reaction of linseed oil (LO) was performed. The FTIR spectra were obtained for both the raw material (LO) and the corresponding epoxide (ELO), which were

consistent with those reported by González-Martínez et al (26). The most representative vibration signals of LO (Figure 1a) correspond to the carbonyl group of ester at 1736 $cm^{-1}$ (C=O). The double bonds (DB) signals are found at 3021 $cm^{-1}$ (=C-H), 1652 $cm^{-1}$ (C=C), and 720 $cm^{-1}$ ($HC=CH_{cis}$). The other vibrational bands correspond to the ester carbonyl (1736 and 1159 $cm^{-1}$), methyl (2922, 1456, and 1377 $cm^{-1}$), and methylene (2852 and 719 $cm^{-1}$). In the infrared spectrum of ELO (Figure 1b), the vibrational signals of the epoxy ring are identified at 1250 and 823 $cm^{-1}$ (C-O-C), the latter being the most representative. The FTIR technique allowed qualitatively verifying the ELO formation from LO, through the disappearance of DB signals and in turns the appearance of bands corresponding to epoxy rings as previously reported. [25-27].

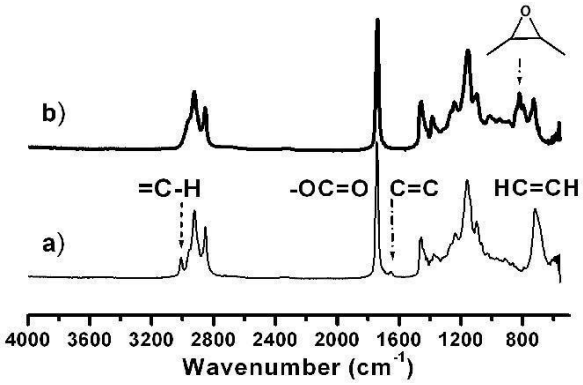


*Figure 1.* FTIR spectra of: a) Linseed Oil; b) Epoxidized linseed.
Source: Own elaboration

Subsequently, for ELO polymerization reaction was added ATF as a catalyst. The FTIR spectrum of the polymerization product is shown in Figure 2a. The signals corresponding to the C-O ether bonds formed due to the opening of the oxirane ring is at 1150 $cm^{-1}$. However, the signals corresponding to the oxirane groups are still visible, indicating that, under these conditions, the polymerization reaction is not complete. As it is a mass polymerization, the viscosity increases as the reaction progresses, reducing the mobility of the reactive agents.

The crosslinking product between ELO and BFA was studied using FTIR spectroscopy, which is shown in Figure 2c. The signals corresponding to the oxirane ring (823 $cm^{-1}$) disappeared because of the ring opening. Broadening of the 1000–1800 $cm^{-1}$ indicates the new C-O ether bonds formed during the curing reaction. Additionally, signals at 1612, 1594, 1510, and 833 $cm^{-1}$ corresponding to the aromatic ring from FBA are also evidenced.

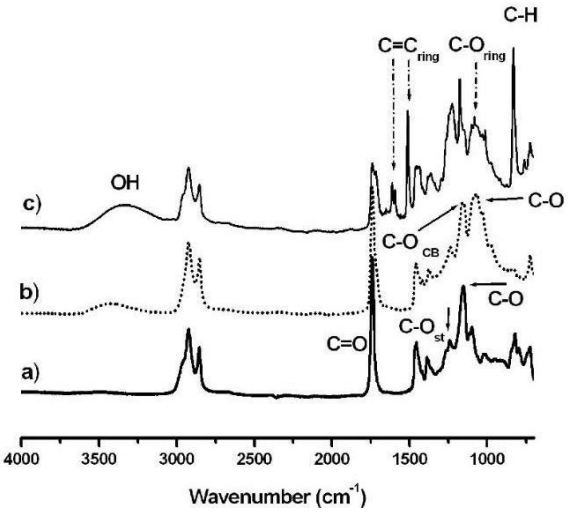


*Figure 2.* FTIR spectrum of: a) ELO resin; b) ELO-Carbon black (CB) resin; c) ELO-Bisfenol A (BFA) resin.
Source: Own elaboration

As mentioned previously, CB is mainly used as reinforcement particles in polymers because it provides UV radiation protection at low cost. CB is mostly composed of elemental carbon; however, different oxygenated functional groups such as phenols, carboxylics, and quinolics can be found on the surface (28), and the possibility of carbon bonds formed between CB and ELO in presence of ATF was investigated. The sample spectrum consists of ELO with CB (Figure 2b).

With BFA, in the presence of CB, the main peaks related to the epoxide groups were not observed, indicating the epoxide ring opening. By adding CB to the epoxy resin, a new band observed around 3440 $cm^{-1}$ was attributed to the -OH group from CB particles. Both the methylene groups (2923 and 2850 $cm^{-1}$) and the esters carbonyl

bonds (1740 $cm^{-1}$) of amorphous CB are overlapped with the signals of ELO bonds. A new sharp and high-intensity peak observed at 1064 $cm^{-1}$ is related to the C-O bonds from the -OH groups in phenols. Therefore, this suggests that a potential chemical interaction occurred between CB with the epoxy ring. Furthermore, it is possible to consider that, in the curing reaction with CB, functional groups present on the CB surface which play an important role for the CB particles are covalently bonded to the ELO matrix (29).

As mentioned previously, introducing new eco-friendly coatings is one of the main challenges; hence the objective of polymerizing ELO with crosslinking agents (BFA) and/or with reinforcements (CB) is to improve adhesion and corrosion resistance of new organic coating on a galvanized steel plate. Additionally, the polymerization can be performed at low temperature to decrease production costs by using the cationic catalyst (ATF) (30). Following the detachment adhesion measurement method, adhesion tests were conducted. The adhesion levels designated to the inspected material based on adhesion failures are shown in Table 2.

*Table 2*. Classification of adhesion level, according to ASTM D3359-02.

| Classification | Description |
|---|---|
| 5A | No peeling |
| 4A | Peel or remove traces along the incisions |
| 3A | Irregular removal along incisions up to 1.6 mm |
| 2A | Irregular removal along incisions up to 3.2 mm |
| 1A | Removing most of the X area under the tape |
| 0A | Removal beyond the X area |

*Source: ASTM D3 359 - 02*

According to the ASTM D3359-02 test, the adhesion test of the crosslinked polymers on the galvanized steel plates acquire an adherence level. Method A described in the test, known as the 3M test, applies to finished products, inspections during production, and also inspections before shipment. Table 3 shows the adhesion results obtained for the different coatings. In all cases, the curing conditions were for 30 min and temperature range of 50–80°C.

*Table 3*. Coating adhesion results (Norm ASTM D3359-02)

| Sample | Result | Observations |
|---|---|---|
| ELO resin | 2A | Between resin and substrate |
| ELO-BFA resin | 5A | No detachment |
| ELO-CB resin | 5A | No detachment |
| ELO-BFA-CB resin | 5A | No detachment |

*Source: Own elaboration*

For ELO polymer, the adhesion results showed detachment failures between the first layer and the substrate. This result suggests that the coating has low adhesion as shown in Figure 3a. In Figure 3, there are two regions framed with green and red colors. The green color indicates the coating and the red color indicates the fraction of the uncoated plate. The polymeric coating (Figure 3a) has a translucent, semiglossy appearance, and irregular detachment was observed along the defined area after adhesion tests. Therefore, the low adhesion of ELO polymer makes it difficult to apply in certain specific areas. This deficiency in the adhesion capacity is because there are only interactions at the interface between the phenoxy oxygen atoms and the Zn atoms from the substrate surface (Scheme 1). That is, only secondary bonds that may include London dispersion forces as well as Van der Waals forces of dipole-dipole type are involved (1,31).

Generally, the polymer absorption on the surface of the galvanized steel plate is a function of both the surface properties of the substrate and the molecular charge of the polymer (32). Therefore, options should be proposed to improve the epoxy resin properties by incorporating substances that allow obtaining pore-free or low-porosity coatings, which form uniform surfaces with good adherent properties. [31]

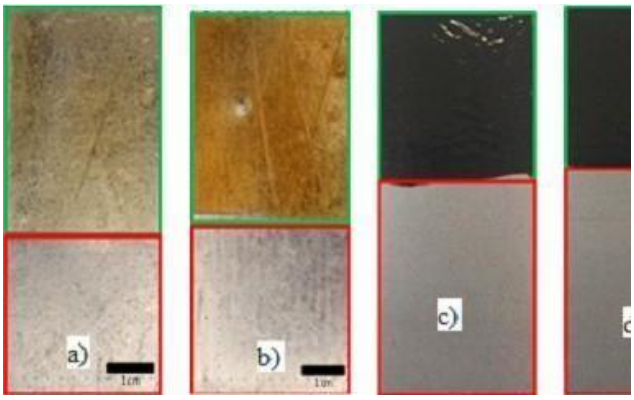


*Figure 3*. Physical appearance of coated sheets after adhesion test: a) ELO resin; b) ELO-BFA resin; c) ELO-CB resin; d) ELO-BFA-CB resin.
Source: Own elaboration

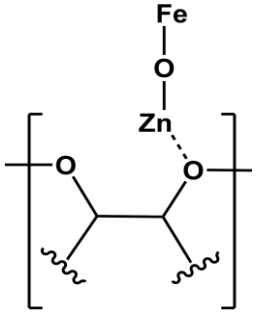


*Scheme 1*. Adhesion between ELO and Zinc substrate represented by secondary bonds.

Source: Own elaboration

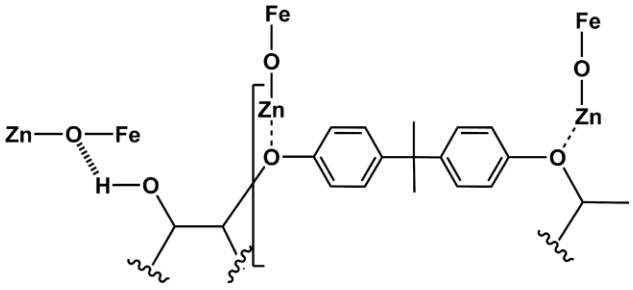


*Scheme 2*. Adhesion between ELO and Zinc substrate by hydrogen bonds.
Source: Own elaboration

Generally, the polymer absorption on the surface of the galvanized steel plate is a function of both the surface properties of the substrate and the molecular charge of the polymer (32). Therefore, options should be proposed to improve the epoxy resin properties by incorporating substances that allow obtaining pore-free or low-porosity coatings, which form uniform surfaces with good adherent properties. [31]

The adherence results corresponding to ELO-BFA coatings exhibit a high level corresponding to level 5A. Therefore, the polymers did not show a deficiency in the adhesion properties because the addition of BFA allowed improving the adhesion properties of the crosslinked polymers on the galvanized steel plates. These coatings had a rigid consistency to the touch, having a translucent semigloss with a yellowish tone. The adhesive capacity of ELO coating has been observed to improve considerably when crosslinked with BFA. The polar group (hydroxyl) presence in the polymer chain improved adhesion with the substrate due to hydrogen bond formation (Scheme 2). Generally, most organic coatings adhere to metals by hydrogen and secondary bonds. The adhesion strength of epoxy resins on metal substrate is a function of the amount of hydroxyl group present in the polymer chain (5, 18, 33).

Similar results were for ELO-CB and ELO-BFA-CB coatings. The adhesion results of both matrices showed a level equal to 5A because CB acts as reinforcement, allowing improving the surface properties and the adhesion of the respective coatings. Furthermore, the ELO matrix in CB presence produced C-O and C-H bonds as observed in the FTIR spectrum (Figure 3b). These chemical bonds can promote both hydrogen bonds and Van der Waals forces, improving the interaction at the interface between the polymeric

matrix and the substrate surface (29, 34, 35). Both systems exhibited stiff consistency to the touch, semigloss black coloration corresponding to the addition of CB. However, compared to the coating with only CB, the ELO-BFA-CB matrix showed more uniform distribution. Therefore, it can be suggested that aromatic ring presence in the polymeric matrix allows CB particles to decrease the tendency to agglomerate.

The corrosion resistance performance of the different coatings was evaluated by a qualitative test inside a salt spray chamber. Under the norm ASTM-B117, in a corrosive environment inside the chamber (Table 1), the physical appearance of the sheet was visually evaluated after 240 h of exposure. The results of the salt spray chamber test are in Table 4.

*Table 4*. Salt spray chamber results (Norm ASTM-B117)

| Substrate | Coating | Results |
|---|---|---|
| Commercial galvanized steel sheet | Uncoated | Signs of white and red corrosion |
| | ELO resin | Signs of white corrosion and delamination |
| | ELO-BFA resin | Small signs of corrosion, no delamination |
| | ELO-CB resin | No corrosion signs |
| | ELO-BFA-CB resin | No corrosion signs |

Source: Author observations according ASTM – B117 test

For comparison, Figure 4a illustrates the optical image of the uncoated sheet after the corrosion test. As expected, the generation of large amounts of white and red corrosion over the completely uncoated surface is evident. Figure 4b shows the behavior of the substrate coated only with ELO. The results demonstrated that there are signs of white corrosion and strong delamination of the sheet coating, as observed also by Moura, J. H. L. et al. (1). Furthermore, there is damage to the adhesive characteristics caused by water and ion penetration at the interface between the coating and sheet plate because poor adhesion properties of ELO on the substrate were also obtained (36). Previous studies have revealed that strong adhesion of the coating on the substrate is necessary for good anticorrosion properties of coating. When metal is subjected to a corrosive environment, it will corrode if the adhesion is inadequate. Inadequate adhesion will promote coating failure and corrosion problems if the substrate is exposed to a corrosive environment (5, 30, 37).

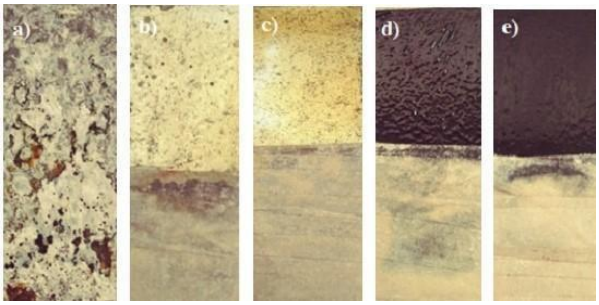


*Figure 4.* Physical appearance of the different substrates after 240 h into a salt spray chamber: a) Uncoated; b) Coated with ELO; c) Coated with ELO-BFA; d) Coated with ELO-CB; e) Coated with ELO-BFA-CB.

Source: Own elaboration

The results of the ELO-BFA-coated sheet show no signs of delamination as shown in Figure 4c. Furthermore, there are some signs of corrosion, although they are minor compared to those exhibited by the ELO coating. This improvement in both adhesive and anticorrosive properties is because the coating is formed with a greater degree of crosslinking due to the OH groups on BFA and higher hydrophobic character conferred by the aromatic rings. Higher crosslink density means a more compact structure and therefore better corrosion protection. As mentioned previously, some signs of corrosion were observed; this is possibly because the coating obtained exhibited a certain porosity degree that

is not effective in protecting the substrate from corrosive agents (1, 31, 38, 39). Finally, with the addition of CB to the coatings (Figure 4d and Figure 4e), dark and denser semigloss coatings are formed. For the ELO-BFA-CB system, compared to ELO-CB coating, the surface appears uniform. The functional groups of BFA distribute the charge and reduce the tendency of CB to agglomerate, allowing a uniform distribution of the coating on the substrate and improving the anticorrosive capacity of the coating (19,31).

Additionally, for both systems, there is a considerable improvement in corrosion resistance properties. One possible explanation is that CB particles increase the polymeric density of coating, reducing the porosity of coating, and since they are present on the surface of various functional groups that could interact with chloride ions; the coating could retain or prevent diffusion towards the substrate, reducing the corrosion phenomenon. Therefore, the coating's ability to protect the substrate from corrosion is also a function of how accessible it is for ions to reach the interface between the coating and substrate. [40-42].

## 4. Conclusions

Using ATf as an acid catalyst, it was possible to polymerize ELO, BFA, and CB on Fe-Zn sheets in a temperature range of 50–80°C, catalyst concentration of 0.01M, and 30 min of reaction. The curing time was monitored by FTIR, quantifying the area under the curve of the oxirane bonds. It evidenced the ELO polymerization due to the decrease in the signal strength at 795 and 823 $cm^{-1}$, corresponding to the vibrational bands of epoxide groups. As well as, the signals of hydroxyl groups (3200–3500 $cm^{-1}$) and C=C of the aromatic ring (1612, 1594, and 1510 $cm^{-1}$) in presence of BFA. While using CB, the reaction with ELO was confirmed by increasing the signal of C-O bonds (1160 $cm^{-1}$) and also the -OH bonds.

Regarding the adhesion tests, although ATF allows the ELO crosslinking on the Fe-Zn sheets, it does not show good adhesion on the substrate surface. The BFA incorporation showed the best adherence results at 60–70°C because they did not show coating detachment, while the CB incorporation provided good adherence, regardless of the reaction temperature. Additionally, the CB incorporation allows obtaining a uniform coating, improving the physical appearance. The improvement in resin adhesion using crosslinking agents is probably due to the hydroxyl groups generated during the reaction. It is possible that the formation of hydrogen bonds and Van der Waals forces between the resin and Fe-Zn sheets is promoted. In the resin polymerized only with ELO, the adhesion is lower because the amount of the hydroxyl group is minor (less polar character).

Preliminary weathering tests on the Fe-Zn sheets without coating showed evidence of corrosion. However, the substrates of ELO with the crosslinking agent (BFA) and reinforcement (CB) resisted a weathering test according to norm ASTM-B117.

A biobased resin was polymerized at low temperature on commercial galvanized sheets, which impacts caring for the environment, by using coatings from natural-renewable sources, giving an alternative to substitute petroleum-derived materials.

## 5. Funding Statement and/or acknowledgement

Authors thank CONACYT for the scholarship granted to the student (701376). To CONACyT Basic Sciences Project A1-S-33899, registration in Secretary for Research and Advanced Studies of UAEM 4945/2019C and 4965/2020CIB.

## 6. References


1. Moura JHL, Heinen M, Da Silva, RC, Martini EM, Petzhold CL. Reinforcing anticorrosive properties of biobased organic coatings through chemical functionalization with amino and aromatic groups. Prog Org Coat**.** 2018 dec; 125:372–83. doi:10.1016/j.porgcoat.2018.09.021

2. Loto RT, Olowoyo O. Corrosion inhibition properties of the combined admixture of essential oil extracts on mild steel in the presence of $SO_4^{2-}$ anions. S Afr J Chem Eng. 2018 dec; 26:35-41 doi:10.1016/j.sajce.2018.09.002

3. Thanawala K, Mutneja N, Khanna AS, Singh Raman RK. Development of self-healing coatings based on linseed oil as autonomous repairing agent for corrosion resistance. Materials 2014 nov; 7(11):7324-38. https://doi.org/10.3390/ma7117324

4. Gharda N, Galai M, Saqalli L et al. Linseed oil as a novel eco-friendly corrosion inhibitor of carbon steel in 1 M HCl. Surf Rev Lett. 2019 feb; 26(2):1-11. doi:10.1142/S0218625X18501482

5. Sharma N, Sharma S. Anticorrosive coating of polymer composites: A review. Mater Today: Proc. 2020 dec; 44(6):4498-4502. doi:10.1016/j.matpr.2020.10.726

6. Sharmin E, Zafar F, Akram D, Alam M, Ahmad S. Recent advances in vegetable oils based environment friendly coatings: A review. Ind Crops Prod. 2015 dec; 76:215–29. doi:10.1016/j.indcrop.2015.06.022

7. Raja PB, Sethuraman MG. Natural products as corrosion inhibitor for metals in corrosive media - A review. Mater Lett. 2008 jan; 62(1):113-16. doi:10.1016/j.matlet.2007.04.079

8. Njoku DI, Cui M, Xiao H, Shang B, Li Y. Understanding the anticorrosive protective mechanisms of modified epoxy coatings with improved barrier, active and self-healing functionalities: EIS and spectroscopic techniques. Sci Rep. 2017 nov; 7(15597):1-15. doi:10.1038/s41598-017-15845-0

9. Moradi M, Yeganeh H, Pazokifard S. Synthesis and assessment of novel anticorrosive polyurethane coatings containing an amine-functionalized nanoclay additive prepared by the cathodic electrophoretic deposition method. RSC Adv. 2016 mar; 6(33):28089-102. doi:10.1039/C5RA26609B

10. Sørensen PA, Kiil S, Dam-Johansen K, Weinell CE. Anticorrosive coatings: A review. J Coat Technol Res. 2009 jan; 6(4):135-76. doi:10.1007/s11998-008-9144-2

11. Chaudhari AB, Tatiya PD, Hedaoo RK, Kulkarni RD, Gite VV. Polyurethane prepared from neem oil polyesteramides for self-healing anticorrosive coatings. Ind Eng Chem Res. 2013 jul; 52(30):10189-97. doi:10.1021/ie401237s

12. Karmakar G, Ghosh P, Sharma BK. Chemically modifying vegetable oils to prepare green lubricants. Lubricants. 2017 nov; 5(4):1-17. doi:10.3390/lubricants5040044

13. Lligadas G, Ronda JC, Galiá M, Cádiz V. Renewable polymeric materials from vegetable oils: A perspective. Mater

Today. 2013 sep; 16(9):337-43. doi:10.1016/j.mattod.2013.08.016

14. Shen Y, Wu Z, Tao J, et al. Spraying preparation of eco-friendly superhydrophobic coatings with ultralow water adhesion for effective anticorrosion and antipollution. ACS Appl Mater Interfaces. 2020 may; 12(22):25484-93. doi:10.1021/acsami.0c06074

15. Ataei S, Khorasani SN, Neisiany RE. Biofriendly vegetable oil healing agents used for developing self-healing coatings: A review. Prog Org Coat. 2019 apr; 129:77-95. doi:10.1016/j.porgcoat.2019.01.012

16. Majeed AH, Hamza MS, Kareem HR. Effect of adding nanocarbon black on the mechanical properties of epoxy. Diyala J Eng Sci. 2014 mar; 07(1):94–108.

17. Mustata FR, Tudorachi N, Bicu I. Epoxy resins cross-linked with bisphenol a/methylenedianiline novolac resin type: Curing and thermal behavior study. Ind Eng Chem Res. 2012 jun; 51(25):8415-24. doi: 10.1021/ie202909s

18. Alam M, Akram D, Sharmin E, Zafar F, Ahmad S. Vegetable oil based eco-friendly coating materials: A review article. Arab J Chem. 2014 sep; 7(4):469–79. doi:10.1016/j.arabjc.2013.12.023

19. Zhang C, Garrison TF, Madbouly SA, Kessler MR. Recent advances in vegetable oil-based polymers and their composites. Prog Polym Sci. 2017 aug; 71:91-143. doi:10.1016/j.progpolymsci.2016.12.009

20. Verma C, Olasunkanmi LO, Akpan ED et al. Epoxy resins as anticorrosive polymeric materials: A review. React Funct Polym. 2020 nov; 156:1-46. doi:10.1016/j.reactfunctpolym.2020.104741

21. Etika KC, Liu L, Hess LA, Grunlan JC. The influence of synergistic stabilization of carbon black and clay on the electrical and mechanical properties of epoxy composites. Carbon. 2009 nov; 47(13):3128–36. doi:10.1016/j.carbon.2009.07.031

22. Verma A, Baurai K, Sanjay MR, Siengchin S. Mechanical, microstructural, and thermal characterization insights of pyrolyzed carbon black from waste tires reinforced epoxy nanocomposites for coating application. Polym Compos. 2020 jan; 41(1):338–49. doi:10.1002/pc.25373

23. Dehonor-Márquez E, Vigueras-Santiago E, Hernández-López S. Thermal study of aluminum trifluoromethyl sulfonate as effective catalyst for the polymerization of epoxidized linseed oil. Phys Chem. 2019 aug; 9(1):1-7. doi: 10.5923/j.pc.20190901.01

24. Williams DBG, Cullen A. $Al(OTf)_3$-mediated epoxide ring-opening reactions: toward piperazine-derived physiologically active products. J Org Chem. 2009 dec; 74(24):9509-12. doi:10.1021/jo9020437

25. Dehonor-Márquez E, Nieto-Alarcón JF, Vigueras-Santiago E, Hernández-López S. Effective and fast epoxidation reaction of linseed o,il using 50 wt% hydrogen peroxyde. Am J Chem. 2018 nov; 8:99–106. doi:10.5923/j.chemistry.20180805.01

26. González-Martínez DA, Vigueras-Santiago E Hernández-López S. Yield and selectivity improvement in the synthesis of carbonated linseed oil by catalytic conversion of carbon dioxide. Polymer.

2021 mar; 13(6):1-16. doi:10.3390/polym13060852

27. López-Téllez G, Hernández-López S, Vigueras-Santiago E. Characterization of linseed oil epoxidized at different percentages. Superf y Vacío. 2009 mar; 22(1):5-10.

28. Hernández-López S, Vigueras-Santiago E. Acrylated-epoxidized soybean oil-based polymers and their use in the generation of electrically conductive polymer composites. In: El-Shemy H, editor. Soybean - Bio-Active Compd. IntechOpen; 2013, pp. 231-63. doi:10.5772/52992

29. Tsubokawa N. Functionalization of carbon black by surface grafting of polymers. Prog Polym Sci. 1992 may; 17(3):417-70. doi:10.1016/0079-6700(92)90021-P

30. Asemani HR, Ahmadi P, Sarabi AA, Eivaz M. Effect of zirconium conversion coating: adhesion and anti-corrosion properties of epoxy organic coating containing zinc aluminum polyphosphate (ZAPP) pigment on carbon mild steel. Prog Org Coat. 2016 may; 94:18-27. doi:10.1016/j.porgcoat.2016.01.015

31. Deyab MA, Awadallah AE. Advanced anticorrosive coatings based on epoxy/functionalized multiwall carbon nanotubes composites. Prog Org Coat. 2020 feb; 139:1-5 https://doi.org/10.1016/j.porgcoat.2019.105423

32. Mofidabadi AH, Bahlakeh G, Ramezanzadeh B. Explorations of the adhesion and anti-corrosion properties of the epoxy coating on the carbon steel surface modified by $Eu_2O_3$ nanostructured film. J Mol Liq. 2020; 1-14. doi:10.1016/j.molliq.2020.113658

33. Kurbanova R, Okudan A, Mirzaoğlu R, et al. Effects of the functional groups of polystyrene on its adhesion improvement and corrosion resistance. J. Adhes. Sci. Technol. 1998 apr; 12(9):947-55. doi:10.1163/156856198X00560

34. Zhang W, Blackburn RS, Dehghani-Sanij AA. Carbon black reinforced epoxy resin nanocomposites as bending sensors. J Compos Mater. 2009 feb; 43(4):367-76. doi:10.1177/0021998308099308

35. Gantayat S, Rout D, Swain SK. Carbon nanomaterial–reinforced epoxy composites: A review. Polym-Plast Technol Eng. 2018 apr; 57(1): 1-16. doi:10.1080/03602559.2017.1298802

36. Ramezanzadeh M, Bahlakeh G, Ramezanzadeh B, Rostami M. Mild steel surface eco-friendly treatment by neodymium-based nanofilm for fusion bonded epoxy coating anti-corrosion/adhesion properties enhancement in simulated seawater. J Ind Eng Chem. 2019 apr; 72:474-90. doi:10.1016/j.jiec.2019.01.003

37. Gao X, Yan R, Lv Y, Ma H, Ma H. In situ pretreatment and self-healing smart anti-corrosion coating prepared through eco-friendly water-base epoxy resin combined with non-toxic chelating agents decorated biomass porous carbon. J Clean Prod. 2020 sep; 266:1-13. doi:10.1016/j.jclepro.2020.121920

38. Liu B, Fang ZG, Wang HB, Wang T. Effect of cross linking degree and adhesion force on the anti-corrosion performance of epoxy coatings under simulated deep sea environment. Prog Org Coat. 2013 dec; 76(12):1814–18. doi:10.1016/j.porgcoat.2013.05.022

39. Zhang C, Huang KC, Wang H, Zhou Q. Anti-corrosion non-isocyanate polyurethane polysiloxane organic/inorganic hybrid coatings. Prog Org Coat. 2020 nov; 148:1-8. doi:10.1016/j.porgcoat.2020.105855

40. Alagi P, Ghorpade R, Jang J, et al. Controlled hydroxyl functionality of soybean oil-based polyols for polyurethane coatings with improved anticorrosion properties. Macromol Res. 2018; 26:696-703. doi:10.1007/s13233-018-6104-2

41. Pan L, Ding W, Ma W, et al. Galvanic corrosion protection and durability of polyaniline-reinforced epoxy adhesive for bond-riveted joints in AA5083/Cf/epoxy laminates. Mater Des. 2018 dec; 160:1106–16. doi:10.1016/j.matdes.2018.10.034

42. Alagi P, Ghorpade R, Jang J, et al. Functional soybean oil-based polyols as sustainable feedstocks for polyurethane coatings. Ind Crops Prod. 2018 mar; 113:249-58. doi:10.1016/j.indcrop.2018.01.041